Cardiovascular Engineering and Technology, Vol. 10, No. 1, March 2019 *(© 2018)* pp. 112–123
https://doi.org/10.1007/s13239-018-00389-9

Estimation of Biomechanical Properties of Normal and Atherosclerotic Common Carotid Arteries

EFFAT SOLEIMANI,[1] MANIJHE MOKHTARI-DIZAJI,[1] NASSER FATOURAEE,[2] and HAZHIR SABERI[3]

[1]Department of Medical Physics, Faculty of Medical Sciences, Tarbiat Modares University, Tehran, Iran; [2]Department of Medical Engineering, Faculty of Medical Engineering, AmirKabir University of Technology, Tehran, Iran; and [3]Department of Radiology, Imaging Center of Imam Khomeini Hospital, Tehran University of Medical Sciences , Tehran, Iran

(Received 4 April 2018; accepted 12 October 2018; published online 24 October 2018)

Associate Editors Dr. Ajit P. Yoganathan & Dr. Frank Gijsen oversaw the review of this article.

Abstract

Purpose—We developed a modified Kelvin model so that the periodic changes of the arterial intima–media thickness (IMT) over the cardiac cycle were involved. Modified model was implemented for carotid artery, solved *via* a parameter optimization technique and biomechanical parameters of the model.

Methods—Consecutive ultrasonic images of the common carotid artery of 30 male patients including 10 healthy subjects, 10 subjects with mild and 10 subjects with sever stenosis were recorded and processed offline. Temporal changes of the internal diameter and IMT were extracted using a combined maximum gradient and dynamic programming algorithm. The blood pressure waveforms were deduced calibrating the internal diameter waveforms using an empirical exponential relationship.

Results—According to the results of the ANOVA statistical analysis, mean values of the zero pressure radiuses, stress relaxation times, elastic moduli and strain relaxation times of the common carotid arteries of three groups were significantly different. Mentioned parameters increased 11, 24, 7 and 6% in patients with mild ($< 50\%$) stenosis and 12, 73, 8 and 61% in the group with sever stenosis ($> 50\%$) relative to healthy group.

Conclusion—Present study can be an indicative of the general state of the vascular system and be used for discriminating atherosclerotic from healthy arteries.

Keywords—Biomechanical properties, Carotid artery, Parameter optimization, Ultrasonic images.

INTRODUCTION

Alterations in the structural and mechanical properties of the blood vessels are thought to be crucial for early manifestation of the atherosclerotic changes, which may serve as indicative markers for future atherosclerotic disease.[14,23]

Increased stiffness of large arteries has been shown to be attributed to cardiovascular morbidity and mortality in a large percentage of the population of patients with hypertension, atherosclerosis and heart diseases.[6,23,27] Furthermore, the *in vivo* noninvasive Young's modulus estimated from the regional stress–strain relationship is proposed to represent the composite stiffness of the arterial wall regarding the effects of the different constituents.[4,5] However, it has been widely known that blood vessels exhibit viscoelastic properties. Consequently, the stress at a typical point of a muscular artery at a given time depends on both the strain at that time and the strain history.[13]

Vessel wall viscoelasticity introduces a phase difference between pressure and wall deformation, which leads to the well-known hysteresis loop.[24,30] Viscoelasticity of the arterial wall is an important source of physical damping and viscous energy dissipation in the carotid artery was reported to be higher under hypertension conditions.[1]

Some studies showed that the elastic increase (stiffening) was related to local pathologies of the arterial system, while wall viscosity change reflects a more general influence of hypertension on large-artery smooth muscle.[18,19] Therefore, characterization of the viscoelastic behavior of the arterial wall as well as the relationship of viscoelasticity and early diagnosis could widen the knowledge of pathological factors that determine the genesis of atherosclerotic plaques.

Address correspondence to Manijhe Mokhtari-Dizaji, Department of Medical Physics, Faculty of Medical Sciences, Tarbiat Modares University, Tehran, Iran. Electronic mail: mokhtarm@modares.ac.ir

Several models have been proposed in order to characterize the viscoelastic properties of the arterial wall under different experimental conditions. Microstructural models[9,12,15,37] are usually based on generalized Maxwell model from which the nonlinear stress–strain relations are derived as the fundamental elastic properties of the artery wall. Structural models are usually complicated, clinically impractical and well-suited for finite element applications.[13,34] That is, availability and fidelity of experimental data in addition to appropriate modeling methods restrict the modeling efforts. Because of the complex temporal changing behavior of the vessel wall submitted to the cyclic physiological hemodynamic conditions, dynamic modeling and analysis of the arterial wall is required.[4] Hirano *et al.*[10] propose a log-linearized arterial viscoelastic model and estimated the arterial stiffness and viscosity *via* circumferential strain and logarithmic blood pressure waveforms of the common carotid artery.

The aforementioned viscoelastic models of the arteries are often based on the concept of pseudo-elasticity theory, which results in integer order viscoelastic models.[8] Another approach to modeling the behavior of arteries is based on fractional-order viscoelastic models, which can be thought of as a large set of weighted integer-order spring/dashpot pairs arranged in parallel.[25]

Several authors have considered the Kelvin model the most suitable to represent the carotid artery dynamic response. Valdez Jasso *et al.*[31] showed that Kelvin model fitted very well to the data from carotid artery for both *ex vivo* and *in vivo* conditions better than the sigmoid and arctangent models.

Currently ultrasound image based methods have been developed to extract the biomechanical parameters of artery wall from the information on the movement of the arterial wall and pressure variations over the cardiac cycle. Balocco *et al.*[3] proposed a non-iterative method to estimate the viscoelastic parameters of a vascular wall Zener model. They measured flow variations and wall displacements with Doppler ultrasound and fitted the theoretical constitutive equations to the experimental measurements to capture fundamental viscoelastic properties of the arterial wall.

It seems, more sophisticated models may provide more accurate estimation of parameter given that higher computation costs. Valdez Jasso *et al.*[32] showed that adding a second relaxation term to the creep function did not improve the estimation data.

The main goals of the present study are in some aspects: first the fundamental Kelvin viscoelastic model is modified to involve the instantaneous changes of IMT of the carotid artery over the cardiac cycle, second a solely ultrasound image processing method is introduced for noninvasively extracting the modified model parameters and finally feasibility of the proposed technique of estimating biomechanical parameters in discriminating the healthy and stenosed carotid arteries is evaluated in three groups of male subjects.

METHODS

– Kelvin model: The standard viscoelastic model of Kelvin (Eq. 1) is known as the simplest model including the effects of arterial wall creep, stress relaxation and hysteresis. In analogy to the periodic distention of the artery wall under cyclic blood pressure, the constitutive equation of the Kelvin model corresponding to the vessel wall deformation is[32]:

$$s(t) + \tau_\sigma \frac{ds(t)}{dt} = \frac{r_0}{Eh}\left(p(t) + \tau_\varepsilon \frac{dp(t)}{dt}\right), \quad s(t) = 1 - \frac{r_0}{r(t)} \tag{1}$$

where S, p and h are radial strain, transmural pressure and intima–media thickness (IMT) respectively. τ_σ, τ_ε, E and r_0 are relaxation time for a fixed stress, relaxation time for a fixed strain, elastic modulus and zero pressure radius of the artery respectively.

Numerous studies have shown that arterial wall thickness represents periodic behavior over the cardiac cycle.[16,21,35] Thus in this study, the fundamental equation of Kelvin model was modified to include the temporal changes of IMT (Eqs. 2 and 3). The modified equation was solved *via* linear nonhomogeneous differential methods:

$$s(t) = \exp\left(-\frac{t}{\tau_\sigma}\right)\left\{s(0) + \int_0^t \frac{r_0}{E\tau_\sigma}\left[\frac{p(x)}{h(x)} + \tau_\varepsilon \frac{p'(x)}{h(x)}\right]\exp\left(\frac{x}{\tau_\sigma}\right)dx\right\} \tag{2}$$

where x is the dummy integral variable and $t = 0$ corresponds to the initial state of the artery deformation (diastole).

By substituting the strain in terms of artery radius and decomposing the integral to sum of trapezoid areas, discrete expression of the instantaneous radius (r(i)) of the artery is achieved as:

$$r(i) = \left\{ \frac{1}{r_o}\left(1 - \exp\left(-\frac{t_i}{\tau_\sigma}\right)\right) + \frac{\exp\left(-\frac{t_i}{\tau_\sigma}\right)}{DR} - \frac{\exp\left(-\frac{t_i}{\tau_\sigma}\right)}{E\tau_\sigma} \sum_{j=2}^{i} \left[a(j)\exp\left(\frac{t(j)}{\tau_\sigma}\right) + a(j-1)\exp\left(\frac{t(j-1)}{\tau_\sigma}\right)\right]\left(\frac{t(j)-t(j-1)}{2}\right) + \tau_\varepsilon\left[b(j)\exp\left(\frac{t(j)}{\tau_\sigma}\right) + b(j-1)\exp\left(\frac{t(j-1)}{\tau_\sigma}\right)\right] \times \left(\frac{t(j)-t(j-1)}{2}\right)\right\}^{-1} \quad (3)$$

where $a = \frac{p}{h}$, $b = \frac{p'}{h}$ and i denotes each of measured data points in the time series of measurements. Given the instantaneous transmural pressure, pressure differentiation and IMT of artery wall as well as internal diameter (radius) are known, Eq. (3) can be solved using an inverse problem method in which a set of initial values are selected for the model parameters. Then an optimization technique is implemented to estimate a set of model parameters which minimizes the least square error between estimated and measured values of the artery radius. That is, the objective cost function is defined as the sum square differences between the instantaneous measured radius and those computed from modified Kelvin model scaled by degrees of freedom (number of data points (n) minus the number of model parameters (n_p)). Optimal parameters (p) are those minimize the cost function.

$$\text{cost function} = \frac{1}{n - n_p}\sum_{i=1}^{n}|R_i - r_i(p)|^2 \quad (4)$$

where R_i and r_i are instantaneous measured and computed radiuses respectively.

In the present study, pattern search algorithm in MATLAB environment was used to compute the subject specific optimal parameters. This algorithm uses a set of vectors (pattern) based on independent parameters of the objective function and basis set to determine the point is to be searched in each iteration.[2] For the current study, initial values for τ_σ, τ_ε and E were obtained from literature, 0.05 (s), 0.025 (s)[32] and 1900 mmHg (250 kPa),[36] respectively. In order to avoid the influence of initial values on the result comparison between groups, we used the same initial values for τ_σ, τ_ε, E for all groups. Whereas the diastolic radius, which is bigger than the true r_0, was taken as initial value for r_0 of each subject. In this study termination conditions of the optimization algorithm were set as follow: maximum number of function evaluation to 10^8, function tolerance to 10^{-5}, maximum number of iterations to 5000, parameter tolerance to 10^{-8}, complete poll to 'on', cache to 'on', cache tolerance to 10^{-5} and mesh tolerance to 10^{-5}.

- Study population: The study group consisted of 30 volunteers. Male subjects of the present study were divided into three groups (mean age 66 years): healthy male volunteers ($n = 10$) without any history of cardiovascular disease, hypertension, smoking or diabetes; male patients ($n = 10$) having mild ($< 50\%$) atherosclerotic plaques in the origin of their internal carotid arteries (ICA) and male patients ($n = 10$) having severe ($> 50\%$) atherosclerotic plaques in the origin of their ICA. Patients were recruited from patients who underwent carotid angiography for the diagnosis or angioplasty at Imaging Center of Imam Khomeini Hospital. Informed consent was taken from all subjects for the examination and the ethical committee of Tarbiat Modares University approved the protocol of the study.
- Ultrasonography: After at least 10 min rest in the supine position, systolic and diastolic blood pressures were taken from left radial arteries of the subjects *via* a calibrated digital sphygmomanometer prior to imaging. Ultrasonic examination was carried out with a Sonoline Antares (Siemens, Germany) ultrasound system equipped with a 5–13 MHz linear transducer. Left common carotid artery of the subjects, 2 cm proximal to the carotid bulb, was scanned longitudinally. AVI format of the consecutive images of the common carotid artery with a frame rate of 30 Hz was transferred to a PC for offline processing. Each recording contained three cardiac cycles. An in-house software was developed in MATLAB environment (Math Works, Natick, MA, USA) to extract consecutive images in BMP format from AVI movies. This software provided the image dimensions (the images were 510×480 pixel^2), image type (B-mode), and pixel dimensions (0.072×0.072 mm^2).

Measurements were taken from the arterial wall on the far side from the transducer because of better reflections due to the interface blood–intima–media layers.[17]

- Data acquisition:
- Diameter and IMT: IMT and internal diameter were measured offline using an edge detection algorithm, designed in Ultrasound Laboratory of Tarbiat Modares University under MATLAB

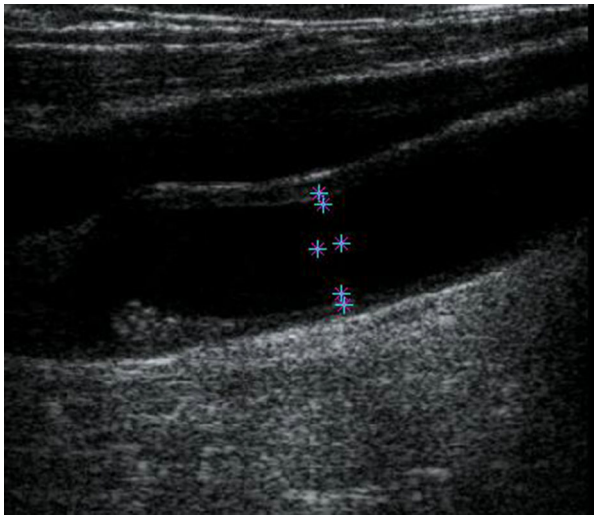

FIGURE 1. An ultrasound image of the stenosed carotid artery and the points (stars) defining the region close to the boundary to be searched by the algorithm.

software to evaluate time rate changes of these parameters from processing consecutive ultrasonic images. Details and validation of this algorithm has been described elsewhere.[28] The first method of edge detection is based on the block-matching algorithm. As long as the brightness intensity is assumed to be constant, given a block of pixels or reference block in the current frame, matching consists in finding the block in the next (or previous) frames that best matches the block in the reference frame. The displacement vector is estimated by matching the information content of a measurement window with that of a corresponding measurement window within a search area, placed in the previous frame. Briefly, this custom written program is a combination of dynamic programming (DP) and maximum gradient (MG) algorithms. In the DP algorithm, the artery boundary is determined by finding an optimal polyline by optimizing a cost function, which includes weighted terms of echo intensity, intensity gradient and boundary continuity within a rectangular region close to the boundary searched. Whereas in the MG algorithm the reference points are placed in the middle of the searching area. Then, the points are connected by lines and a path perpendicular to the boundary is searched and the point of maximum intensity gradient is picked up (Fig. 1).

– Transmural pressure and pressure differentiation: According to the results of literature, diameter waveforms scaled by an exponential calibration formulation treat and are considered as pressure waveforms. Therefore, we assumed that the pressure and diameter waveforms have an exponential relationship[33]:

$$p(t) = p_{\mathrm{d}} \exp\left[\left(\frac{D^2(t) - D_{\mathrm{d}}^2}{D_{\mathrm{s}}^2 - D_{\mathrm{d}}^2}\right) \ln\left(\frac{p_{\mathrm{s}}}{p_{\mathrm{d}}}\right)\right] \qquad (5)$$

where subscripts 's' and 'd' denotes the systole and diastole respectively and D is internal diameter (mm) of the artery.

It has been reported that Gaussian function can best fit and model the carotid artery pressure waveforms.[20] Thus to achieve the mathematically differentiable equation describing the pressure waveform, Gaussian function was fitted to the pressure waveforms resultant from diameter calibration (Eq. 5). Fitting process was carried out using MATLAB fitting techniques in which waveform equation as well as best-fit parameters are determined *via* nonlinear goodness of fit statistics.[22] Since the more the number of fitted parameters is, the higher R^2 becomes without any fit improvement, Adjusted R^2 which is defined as R^2 scaled with respect to degrees of freedom was used as best statistical parameter evaluating goodness of fit.[29] Thereafter, temporal changes of pressure differentiation were extracted by differentiating the Gaussian equation fitted to the pressure curve of each subject. In this study, diastolic blood pressure was assumed to remain constant throughout the arterial tree.[7] To validate the temporal changes of pressure, the systolic and diastolic pressures of the individual Radial artery was extracted. Moreover, according to the findings, pulse pressure (PP) amplification between carotid and radial arteries approximates 10–15 mmHg either in normotensive or hypertensive subjects.[27] Therefore, a mean value of 12 mmHg for amplification between the systolic blood pressures of carotid and radial arteries was considered. Ultimately, instantaneous arterial radius, IMT, transmural pressure and pressure differentiation were replaced in the Eq. (4) and viscoelastic parameters of the modified Kelvin model were deduced *via* aforementioned iterative optimization method. Mean values of the subject specific optimal parameters, resulting in the least cost function, were extracted over three cardiac cycles. The optimization process of one cardiac cycle took 30 s to 5 min for modified viscoelastic model (on a desktop with eight cores of Intel Core i7-2600@3.4 GHz).

– Statistical analysis: Data are reported as mean ± SD analysis of variance (ANOVA) was used to determine the significance of differences between the groups. Differences were consid-

TABLE 1. General characteristics of three groups of the subjects.

	Healthy	Less than 50%	More than 50%	*p* value
Age, years	38 ± 8	66 ± 7	73 ± 5	0.000
SBP, mmHg	125 ± 6	135 ± 24	144 ± 16	0.051
DBP, mmHg	75 ± 5	81 ± 15	86 ± 9	0.078
Heart rate, bpm	74 ± 9	68 ± 9	78 ± 4	0.095
BMI*	26 ± 2	27 ± 2	27 ± 3	0.354
Carotid stenosis (%)	0	24 ± 9	77 ± 16	0.000

SBP, systolic blood pressure, DBP, diastolic blood pressure, BMI, body mass index defined as the body mass divided by the square of the body height.

ered significant when results showing $p < 0.05$ were seen.

RESULTS

General characteristics of study participants are given in Table 1. As it can be seen, patients with higher stenosis percentage are older and have higher blood pressures (p value > 0.050).

Figure 2 shows the ultrasonic images of common carotid artery and the boundaries determined by the algorithm for internal diameter and IMT of a healthy subject (a, b), a subject with $< 50\%$ stenosis (c, d) and a subject with $> 50\%$ stenosis (e, f) in the carotid artery respectively.

Figures 3, 4 and 5 represent the IMT (a) and internal diameter (b) waveforms of the common carotid artery of a healthy, a less than 50% and a more than 50% stenotic subject respectively. The average values of maximum and minimum internal diameter and IMT of the common carotid artery of three groups of subjects are provided in Table 2. Table 2 shows that although there is a mild increase in the internal diameter of the stenosed groups relative to the healthy subjects but IMT increases significantly. Maximum IMT increases 41 and 67% in the groups with less and more than 50% stenosis respectively and minimum IMT increases 55 and 120% in the groups with less and more than 50% stenosis respectively.

Carotid pressure waveform was obtained from exponentially calibrating the internal diameter waveform to the diastolic and systolic pressures of carotid blood pressures, which were obtained from diastolic blood pressure and subtracting 12 mmHg from systolic blood pressure of the radial artery respectively. Gaussian function was fitted to the pressure waveforms resultants from diameter calibration. For one subject of each group of participants, the pressure waveforms resulted from diameter and that from Gaussian fitting is depicted in Figs. 3, 4 and 5(c).

The mean values of Adjusted R^2, for fitting the Gaussian function on the pressure waveform were 0.998 ± 0.001, 0.997 ± 0.003 and 0.997 ± 0.002 respectively for the studied groups including healthy, low risk and high risk subjects. By differentiating the Gaussian function equation fitted to the pressure waveform, the pressure differentiation waveform of individual subjects was achieved. Mean values of the maximum pressure differentiation of three groups of subjects are provided in Table 2. Pressure differentiation waveforms of a healthy, a less than 50% and a more than 50% stenotic subject are presented in Figs. 3, 4 and 5(d), the same subjects of whom the pressure waveforms are depicted in Figs. 3, 4 and 5(c). Internal diameter, IMT, pressure and pressure differentiation waveforms as well as the initial values of the parameters were replaced in the Eq. (4) and the optimization process was carried out. The subject specific optimal parameter set was extracted for all subjects of the groups. Results of the mean values of the optimal parameters describing the viscoelastic behavior of the common carotid artery of healthy and atherosclerotic (stenotic) subjects are summarized in Table 3. The internal radius obtained from modified Kelvin model using the optimal parameters Eq. (3) and the radius resulted from ultrasonic measurement (gradient algorithm) for the same aforementioned subjects are shown in the Figs. 3, 4 and 5(e).

According to the results of the ANOVA statistical analysis, there are significant differences between the zero pressure radiuses of the common carotid artery of three groups (Table 3). Mean values of zero pressure radiuses of the common carotid arteries increased respectively 11 and 12% in patients with mild ($< 50\%$) and significant ($> 50\%$) stenosis in carotid artery relative to the healthy group. Furthermore, with stenosis initiation and its progression, stress relaxation time of the artery wall increases significantly (Table 3). Stress relaxation time of the arterial wall increased 24 and 73% in patients with less and more than 50% stenosis in the internal carotid artery respectively. Moreover, differences between the Young modulus of

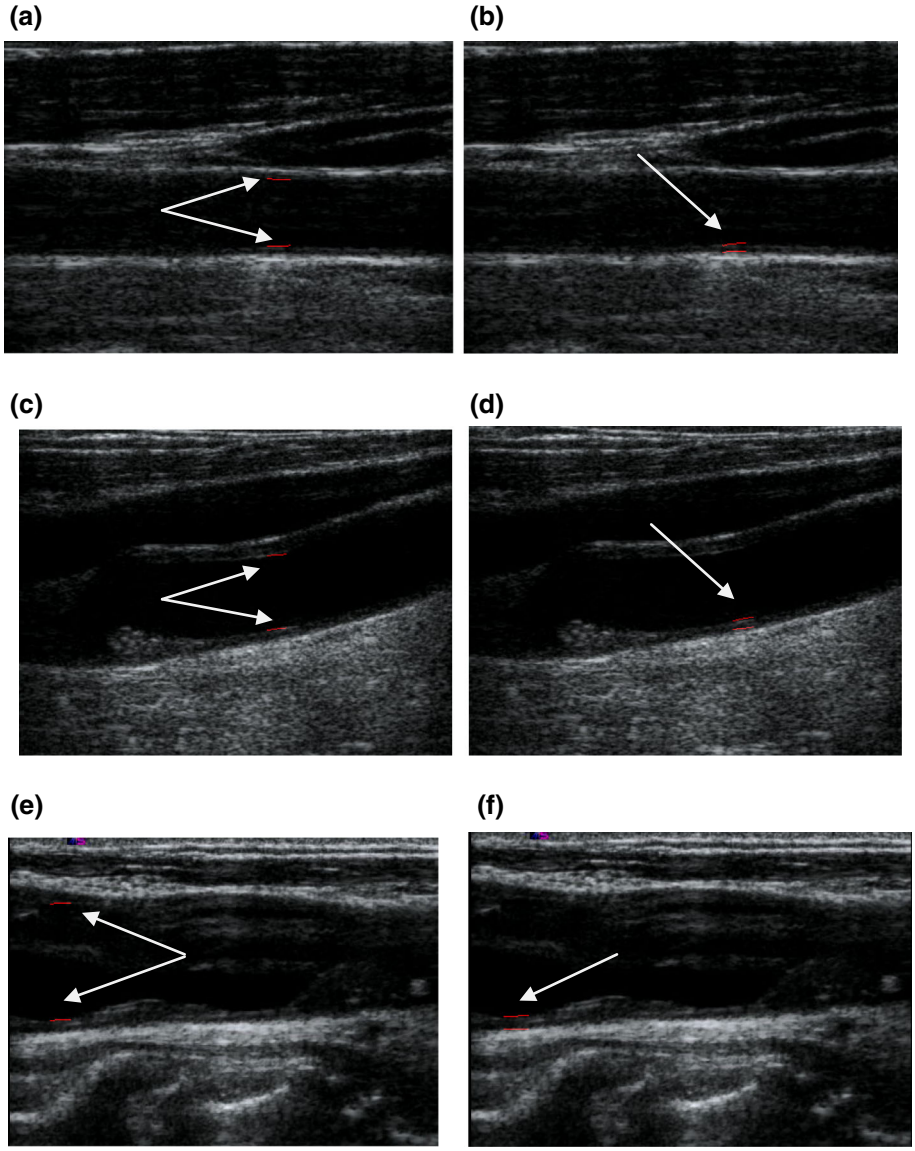

FIGURE 2. Ultrasound images of common carotid artery and the boundaries for internal diameter and IMT of a healthy subject (a, b), a subject with < 50% stenosis (c, d) and a subject with > 50% stenosis (e, f) in the carotid artery respectively.

the arterial wall of the groups are significant ($p < 0.05$). The Young modulus increased 7 and 8% in the groups of less and more than 50% stenosis relative to healthy group respectively.

As it can be seen, statistical analysis showed that mild and severe stenosis (less and more than 50%) in the carotid artery resulted in a significant increase of strain relaxation time of the arterial wall, in which the strain relaxation time increased 41 and 61% in patients with moderate and significant stenosis in carotid artery. The differences of the zero pressure and Young modulus between the stenotic groups were not significant while the differences of the relaxation times were significant between the groups and within the groups.

DISCUSSION

In this study, we developed a modified biomechanical model so that the periodic changes of the arterial IMT over the cardiac cycle were involved. The model variables including artery radius, IMT and blood pressure waveforms were assessed using consecutive ultrasonic images of vessel wall. Feasibility of the proposed technique was examined by applying it in clinical practice for three groups of male patients. Our results reveal that the zero pressure radius increases significantly by atherosclerosis progress (percentage of stenosis) which is in agreement with the results reported in literature in which it has been reported that vessels accommodate changes in blood volume by

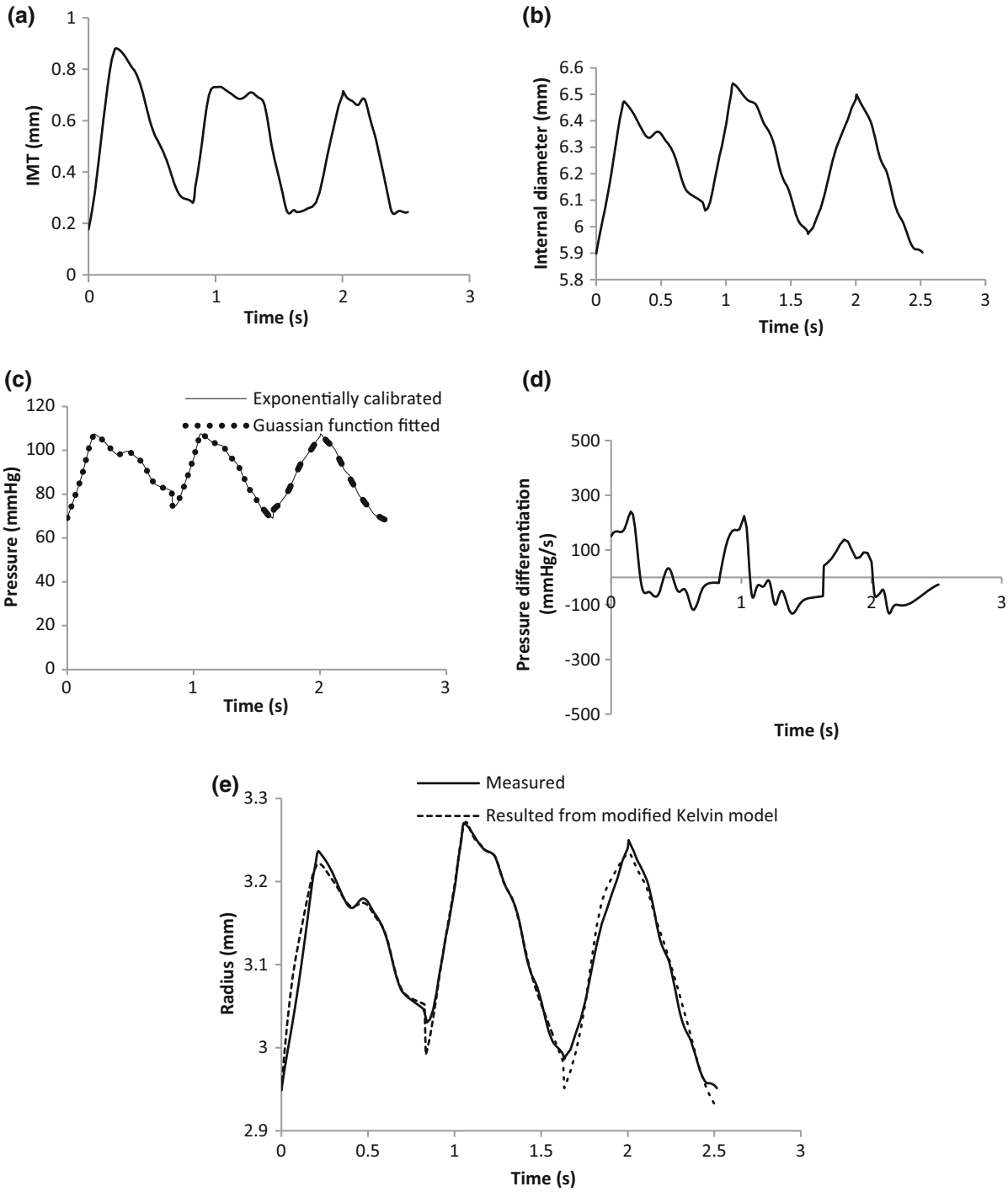

FIGURE 3. Carotid artery IMT (a), internal diameter (b), pressure resulted from exponentially calibrated diameter and that resulted from Gaussian function fitting (c), pressure differentiation (d) and radius resulted from modified Kelvin model overlapped with measured radius (e) waveforms for a healthy subject.

increasing their diameter determining concomitant values of intraluminal pressures.[5] In this study, the group with the highest blood pressure had the largest zero pressure radius.

Since zero-pressure radius is not distinguishable *in vivo*, the proposed method in this study can be used to compute r_0 *in vivo* in studies in which the viscoelastic parameters are objective. The fact that the relaxation time for a fixed strain (τ_ε) is shorter than the relaxation

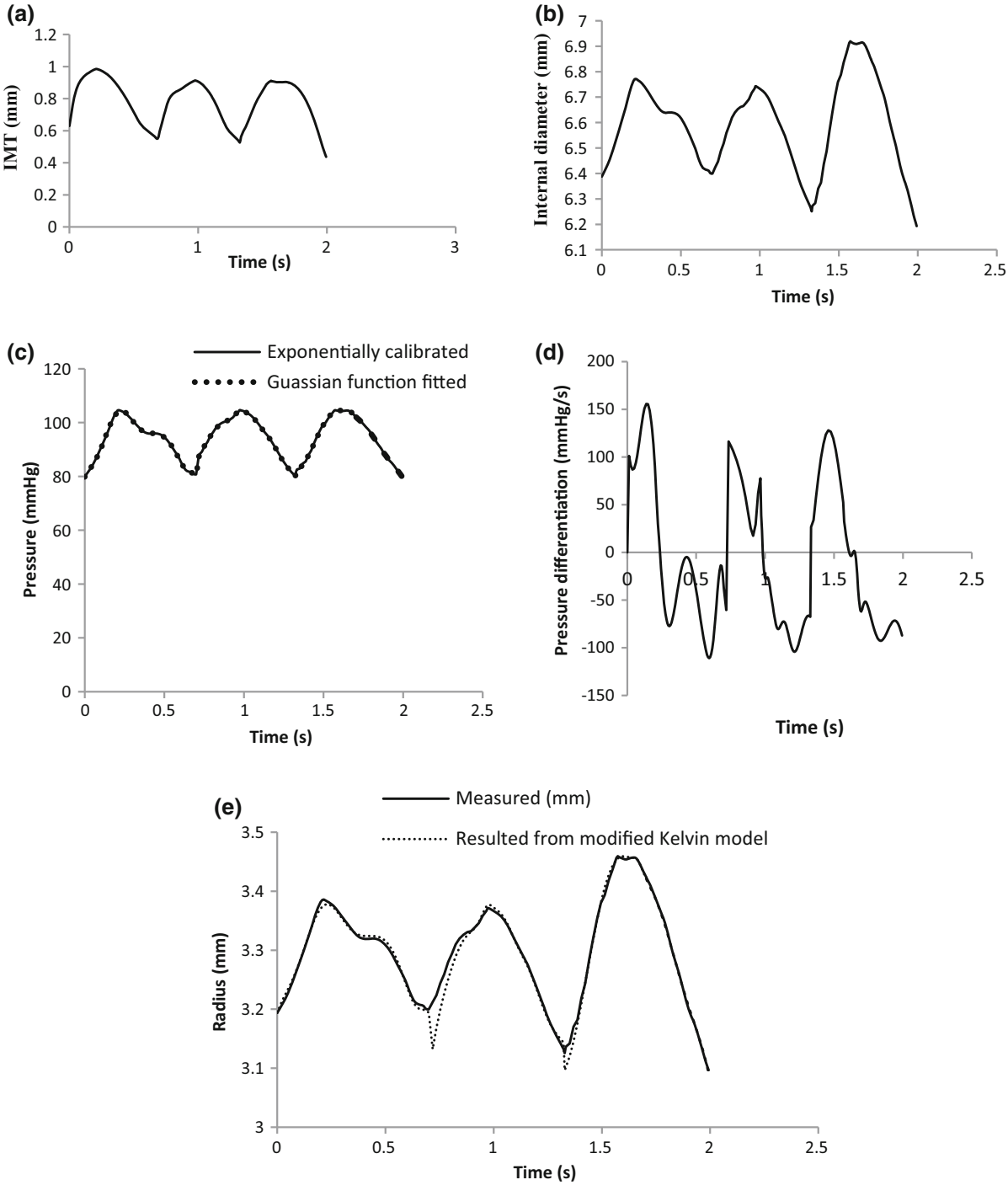

FIGURE 4. Carotid artery IMT (a), internal diameter (b), pressure resulted from exponentially calibrated diameter and that resulted from Gaussian function fitting (c), pressure differentiation (d) and radius resulted from modified Kelvin model overlapped with measured radius (e) waveforms for a subject with < 50% stenosis in carotid artery.

time for a fixed stress (τ_σ) for all biological soft tissues has been noted,[8] to which accordingly we took the initial value of τ_σ to be twice the initial value of τ_ε.

The radiuses resultant from this model quantitatively agreed with the measured ones (Figs. 3, 4 and 5(e)), showing that the accuracy of the method is not particularly affected by changing physiological conditions. Moreover, as can be observed from Figs. 3, 4 and 5(e), total estimation errors are low because this model accurately approximates the kinetic of the carotid artery wall and it fits very well to the carotid artery data of healthy and atherosclerotic subjects.

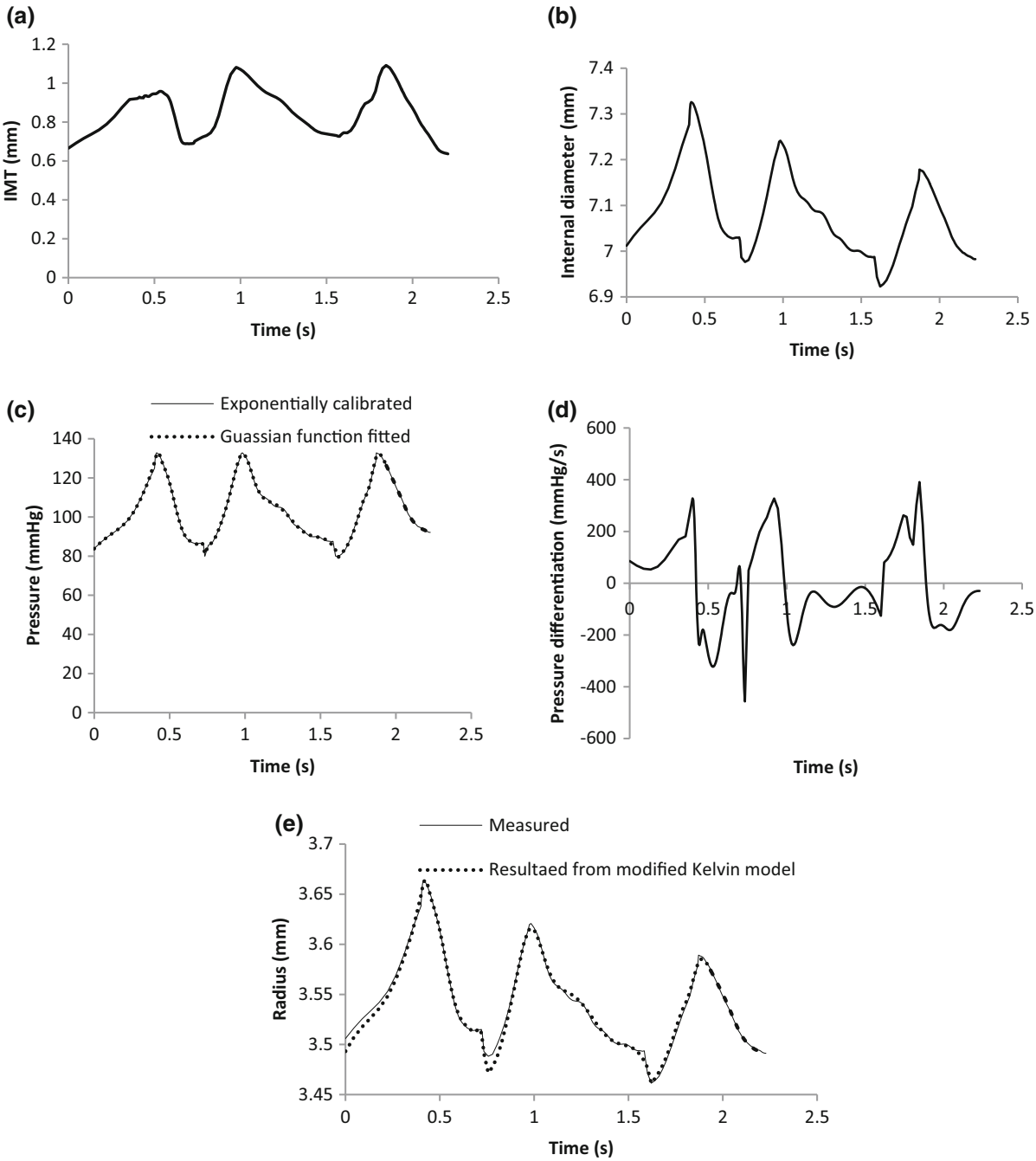

FIGURE 5. Carotid artery IMT (a), internal diameter (b), pressure resulted from exponentially calibrated diameter and that resulted from Gaussian function fitting (c), pressure differentiation (d) and radius resulted from modified Kelvin model overlapped with measured radius (e) waveforms for a subject with > 50% stenosis in carotid artery.

High values of Adjusted R^2 demonstrate that the Gaussian function fitting process does not affect the final estimations and the approximation is reasonable and the errors are low. Results of the study of Valdez-Jasso *et al.*[32] on the elastic and viscoelastic properties of ovine arteries at different anatomical locations showed that the stiffer the artery was, the higher the 'Eh' value was and the longer the relaxation times were. Consistently, in the present study the severer atherosclerotic stenosis percentage was, the higher the Young modulus and the longer the relaxation times became. That is, in the presence of atherosclerotic occlusion the artery responses more slowly to the loading and unloading conditions. Quantitative differences between our results and those of Valdez-Jasso *et al.*[32] may be due to that their study was on ovine

TABLE 2. Mean values of maximum and minimum internal diameter and IMT of the common carotid artery of three groups of subjects included in study.

	Healthy	Less than 50%	More than 50%	*p* value
Max *D* (mm)	6.17 ± 0.64	6.20 ± 0.51	6.35 ± 0.53	0.003
Min *D* (mm)	5.70 ± 0.60	5.68 ± 0.47	6.05 ± 0.51	0.006
Max IMT (mm)	0.61 ± 0.16	0.86 ± 0.15	1.02 ± 0.24	0.000
Min IMT (mm)	0.29 ± 0.09	0.45 ± 0.30	0.64 ± 0.24	0.000
Max pressure differentiation (mmHg/s)	192.88 ± 48.71	187.60 ± 33.54	262.66 ± 68.59	0.000

TABLE 3. Mean values of the optimal parameters describing the viscoelastic behavior of the common carotid artery of three groups of subjects included in study.

	Healthy	Less than 50%	More than 50%	*p* value
r_0 (mm)	2.32 ± 0.25	2.57 ± 0.38	2.59 ± 0.14	0.026
τ_σ (s)	5.8 ± 1.47	7.22 ± 3.22	10.01 ± 4.21	0.006
E (mmHg)	1770.08 ± 157.66	1894.84 ± 126.84	1913.58 ± 86.75	0.034
τ_ε (s)	3.11 ± 0.88	4.37 ± 2.25	5.02 ± 1.75	0.018

arteries and they assumed a constant mean thickness to assess viscoelastic parameters along the blood vessel tree.

The results of study done by Hirano *et al.*[10] indicated that the conventional indicators of arteriosclerosis (stiffness and viscosity) do not differ significantly with or without pre-existing disease, while the modified viscosity differs significantly. In our study, the increase percentages of relaxation times for diseased arteries were much more than those of zero pressure radiuses and elastic modulus which means that the relaxation times might be better indicators of biomechanical changes due to atherosclerosis.

Perdikaris[25] reported that viscoelastic response noticeably affects the pressure wave propagation and the pressure–area hysteresis loops. They showed that the reduction in relaxation time ratios resulted to a significant increase in the local pressure wave in the vessel with the model having lower relaxation time ratio producing a stiffer response and predicting much smaller cross sectional wall displacements. Consistently, in our study, the high-risk group had the highest absolute relaxation times and the highest blood pressure.

The time constants of the model or relaxation times dictate the viscoelastic wall response and are indicators of reciprocal temporal response of the arterial diameter and variations of pressure (creep response or relative damping effect). An elevated value of relaxation time is attributed to a slow response, suggesting an increased buffering effect with an increased attenuation of pressure oscillations.[8] Therefore, it can be stated that using the proposed method of the present study makes it possible to quantitatively assess the temporal buffering response of the arteries in clinical condition. This model estimates some parameters/properties, by providing a good fit to the clinical data. However, this does not necessarily merit the characterisation/estimation of the viscoelastic properties of the artery.

Raghu *et al.*[26] compared the impacts of two different viscoelastic and an elastic wall models on the nonlinear finite element blood flow solver in various idealized and physiological simulations. They reported that hysteresis loops had the most significant differences and were steeper for both viscoelastic models compared to the elastic model. Comparing the performance of our approach with other iterative estimation techniques presented in the literature is difficult because each method uses a different viscoelastic model and the gold standard viscoelastic parameters were not available. Nevertheless, our results revealed that by plaque formation and its progression, changes of relaxation times were considerably more than those of elastic modulus and zero pressure radius and all parameters are able to differentiate pathological cases from healthy arteries. There is a very limited availability of *in vivo* experimental results for most of the arteries. The main reason that may motivate one to evaluate the relaxation times, leveraging on their potential ability to manifest early atherosclerotic changes as a single additional parameter.

This study suffers from several limitations. This study focuses on the common carotid artery, however, estimating the biomechanical parameters for various anatomic locations in an arterial network as well as different plaque constituents and hemodynamic conditions in further studies may increase the understanding of atherosclerotic progression and wall

remodeling. Moreover, the present study was carried out while the subjects were in a relaxed situation (at least 10 min resting before imaging), however, applying the proposed method of the present study while giving stress test to the subjects and extracting the model parameters corresponding to the stress test may provide effective information about dynamic properties of the arteries. Besides, implementing the biomechanical parameters resultant from the method described in this study in modeling the vascular mechanics may take a step forward in vascular biomechanics. Studied groups of subjects were classified according to the stenosis percentage, further studies on blind cohorts may establish the clinical significance of the technique proposed in this study.

The transmural pressure is equal to the difference between the existing intravascular and extravascular pressures whereas the latter pressure cannot be measured *in vivo* and is usually ignored in the models.[12] Another limitation of this study is that the effect of extravascular pressure and tethering (surrounding tissue)[11] which have not been considered.

Moreover, it is well known that arterial stiffness increases with age, beginning in the third decade of life.[6] Although mean age of the groups is significantly different, it was not possible to match the groups in accordance to their ages. Further studies are required to assess the relationship between biomechanical parameters and gender, age, hypertension, etc.

The drawback of iterative methods is that they require a model initialization close to the expected values. Since the approach proposed in the present study is an iterative based, the initial condition employed to solve the iterative process becomes relevant due to unavailability to the actual biomechanical parameters of the normal and atherosclerotic arteries.

For an accurate estimation of the biomechanical parameters, this study implements the *in vivo* realistic data resulted from commonly used diagnostic sonography. No assumption about anatomical geometry, fluid dynamic conditions has been added to the computations. The purpose of the current technique is the estimation of the mechanical alteration of the arterial wall, used for early diagnosis of atherosclerosis evolution.

ACKNOWLEDGMENTS

This study was approved by Faculty of Medical Sciences, Tarbiat Modares University. This work was supported in part by the Iran National Science Foundation (INSF).

CONFLICT OF INTEREST

This study was not funded. This study have no conflict of interest to disclose.

ETHICAL APPROVAL

All procedures performed in studies involving human participants were in accordance with the ethical standards of the Tarbiat Modares University and national research committee and with the 1964 Helsinki declaration and its later amendments or comparable ethical standards.

INFORMED CONSENT

Informed consent was obtained from all individual participants included in the study.

REFERENCES

[1]Armentano, R. L., S. Graf, J. G. Barra, G. Velikovsky, H. Baglivo, R. Sánchez, A. Simon, R. H. Pichel, and J. Levenson. Carotid wall viscosity increase is related to intima-media thickening in hypertensive patients. *Hypertension* 31(1 Pt 2):534–539, 1998.

[2]Audet, C., and J. E. Denid. Analysis of generalized pattern searches. *SIMA J. Optim.* 13(3):889–903, 2003.

[3]Balocco, S., O. Basset, G. Courbebaisse, E. Boni, A. F. Frangi, P. Tortoli, and C. Cachard. Estimation of the viscoelastic properties of vessel walls using a computational model and Doppler ultrasound. *Phys. Med. Biol.* 55(12):355–375, 2010.

[4]Balocco, S., O. Basset, G. Courbebaisse, E. Boni, P. Tortoli, and C. Cachard. Noninvasive Young's modulus evaluation of tissues surrounding pulsatile vessels using ultrasound Doppler measurement. *IEEE Trans. Ultrason. Ferroelectr. Freq. Control* 54(6):1265–1271, 2007.

[5]Bia, D., R. L. Armentano, Y. Zócalo, W. Barmak, E. Migliaro, and E. I. C. Fischer. In vitro model to study arterial wall dynamics through pressure-diameter relationship analysis. *Latin Am. Appl. Res.* 35:217–224, 2005.

[6]Bussy, C., P. Boutouyrie, P. Lacolley, P. Challande, and S. Laurent. Intrinsic stiffness of the carotid arterial wall material in essential hypertensives. *Hypertension* 35(5):1049–1054, 2000.

[7]Cheng, H. M., D. Lang, C. Tufanaru, and A. Pearson. Measurement accuracy of non-invasively obtained central blood pressure by applanation tonometry: a systematic review and meta-analysis. *Int. J. Cardiol.* 167(5):1867–1876, 2013.

[8]Fung, Y. C. Biomechanics: Mechanical Properties of Living Tissues, Chap. 7 (2nd ed.). New York: Springer, p. 277, 1993.

[9]Hariton, I., G. de Botton, T. C. Gasser, and G. A. Holzapfel. Stress-driven collagen fiber remodeling in arterial walls. *Biomech. Model Mechanobiol.* 6(3):163–175, 2007.

[10]Hirano, H., T. Horiuchi, A. Kutluk, Y. Kurita, T. Ukawa, R. Nakamura, N. Saeki, Y. Higashi, S. Hodis, and M. Zamir. Arterial wall tethering as a distant boundary condition. *Phys. Rev. E* 80:51913, 2009.
[11]Hodis, S., and M. Zamir. Arterial wall tethering as a distant boundary condition. *Phys. Rev. E* 80(5):051913, 2009; (1–13).
[12]Holzapfel, A. G., and T. C. Gasser. A new constitutive framework for arterial wall mechanics and a comparative study of material models. *J. Elast.* 61:1–48, 2000.
[13]Holzapfel, G. A., T. C. Gasser, and M. Stadler. A structural model for the viscoelastic behavior of arterial walls: continuum formulation and finite element analysis. *Eur. J. Mech. A* 21:441–463, 2002.
[14]Holzapfel, G. A., and H. W. Weizsäcker. Biomechanical behavior of the arterial wall and its numerical characterization. *Comput. Biol. Med.* 28(4):377–392, 1998.
[15]Horgan, C. O., and G. Saccomandi. A description of arterial wall mechanics using limiting chain extensibility constitutive models. *Biomech. Model. Mechanobiol.* 1:251–266, 2003.
[16]Ilea, D. E., C. Duffy, L. Kavanagh, A. Stanton, and P. F. Whelan. Fully automated segmentation and tracking of the intima media thickness in ultrasound video sequences of the common carotid artery. *IEEE Trans. Ultrason. Ferroelectr. Freq. Control* 60(1):158–177, 2013.
[17]Jegelevicius, D., and A. Lukosevicius. Ultrasonic measurements of human carotid artery wall intima-media thickness. *Ultragras* 2:43–47, 2002.
[18]Khamdaeng, T., J. Luo, J. Vappou, P. Terdtoon, and E. E. Konofagou. Arterial stiffness identification of the human carotid artery using the stress-strain relationship in vivo. *Ultrasonics* 52(3):402–411, 2012.
[19]Labropoulos, N., M. Ashraf Mansour, S. S. Kang, D. S. Oh, J. Buckman, and W. H. Baker. Viscoelastic properties of normal and atherosclerotic carotid arteries. *Eur. J. Vasc. Endovasc. Surg.* 19(3):221–225, 2000.
[20]Liu, C., D. Zheng, A. Murray, and C. Liu. Modeling carotid and radial artery pulse pressure waveforms by curve fitting with Gaussian functions. *Biomed. Signal Process. Control* 8:449–454, 2013.
[21]Loizou, C. P. A review of ultrasound common carotid artery image and video segmentation techniques. *Med. Biol. Eng. Comput.* 52(12):1073–1093, 2014.
[22]Marquardt, D. W. An algorithm for least-squares estimation of nonlinear parameters. *J. Soc. Indust. Appl. Math.* 11:431–441, 1963.
[23]Mattace-Raso, F. U., T. J. van der Cammen, A. Hofman, N. M. van Popele, M. L. Bos, M. A. Schalekamp, R. Asmar, R. S. Reneman, A. P. Hoeks, M. M. Breteler, and J. C. Witteman. Arterial stiffness and risk of coronary heart disease and stroke: the Rotterdam Study. *Circulation* 113(5):657–663, 2006.
[24]Özkaya, N., M. Nordin, D. Goldsheyder, and D. Leger. Fundamentals of Biomechanics Equilibrium, Motion, and Deformation (3rd ed.). New York: Springer, pp. 221–228, 2012.
[25]Perdikaris, P., and G. E. Karniadakis. Fractional-order viscoelasticity in one-dimensional blood flow models. *Ann. Biomed. Eng.* 42(5):1012–1023, 2014.
[26]Raghu, R., I. E. Vignon-Clementel, C. A. Figueroa, and C. A. Taylor. Comparative study of viscoelastic arterial wall models in nonlinear one-dimensional finite element simulations of blood flow. *J. Biomech. Eng.* 133(8):3–14, 2011.
[27]Safar, M. E., and A. Kakou. Carotid and brachial blood pressure: measurements in hypertensive subjects. *J. Rev. Bras. Hipertens.* 5(3):122–124, 2008.
[28]Soleimani, E., M. Mokhtari Dizaji, and H. Saberi. Carotid artery wall motion estimation from consecutive ultrasonic images: comparison between block-matching and maximum-gradient algorithms. *J. Tehran Univ. Heart Center* 6:72–78, 2011.
[29]Soleimani, E., M. Mokhtari-Dizaji, and H. Saberi. A novel non-invasive ultrasonic method to assess total axial stress of the common carotid artery wall in healthy and atherosclerotic men. *J. Biomech.* 48:1860–1867, 2015.
[30]Taber, A. L. Nonlinear Theory of Elasticity, Application in Biomechanics (2nd ed.). Washington: World Scientific Publishing Co., pp. 127–135, 2008.
[31]Valdez-Jasso, D., D. Bia, Y. Zócalo, R. L. Armentano, M. A. Haider, and M. S. Olufsen. Linear and nonlinear viscoelastic modeling of aorta and carotid pressure-area dynamics under in vivo and ex vivo conditions. *Ann. Biomed. Eng.* 39(5):1438–1456, 2011.
[32]Valdez-Jasso, D., M. A. Haider, H. T. Banks, D. Bia, Y. Zocalo, R. L. Armentano, and M. S. Olufsen. Analysis of viscoelastic wall properties in ovine arteries. *IEEE Trans. Biomed. Eng.* 56(2):210–219, 2009.
[33]Vermeersch, S. J., E. R. Rietzschel, M. L. De Buyzere, D. De Bacquer, G. De Backer, L. M. Van Bortel, T. C. Gillebert, P. R. Verdonck, and P. Segers. Determining carotid artery pressure from scaled diameter waveforms: comparison and validation of calibration techniques in 2026 subjects. *Physiol. Meas.* 29(11):1267–1280, 2008.
[34]Wang, Z., N. B. Wood, and X. Y. Xu. A viscoelastic fluid-structure interaction model for carotid arteries under pulsatile flow. *Int. J. Numer. Method Biomed. Eng.* 31(5):e02709–e02720, 2015.
[35]Zahnd, G., M. Orkisz, A. Sérusclat, P. Moulin, and D. Vray. Simultaneous extraction of carotid artery intima-media interfaces in ultrasound images: assessment of wall thickness temporal variation during the cardiac cycle. *Int. J. Comput. Assist. Radiol. Surg.* 9(4):645–658, 2014.
[36]Zhao, S. Z., B. Ariff, Q. Long, A. D. Hughes, S. A. Thom, A. V. Stanton, and X. Y. Xu. Inter-individual variations in wall shear stress and mechanical stress distributions at the carotid artery bifurcation of healthy humans. *J. Biomech.* 35(10):1367–1377, 2002.
[37]Zulliger, M. A., A. Rachev, and N. Stergiopulos. A constitutive formulation of arterial mechanics including vascular smooth muscle tone. *Am. J. Heart Circ. Physiol.* 10:1–39, 2004.